Hindawi
International Journal of Polymer Science
Volume 2023, Article ID 4583522, 6 pages
https://doi.org/10.1155/2023/4583522

Research Article

Preparation of Biodegradable Reduced Graphene Oxide/Agar Composites by *In Situ* Reduction of Graphene Oxide

Mezigebu Belay [1,2]

[1]*Biotechnology Center, Institute of Research and Development, Defense University, Bishoftu 1041, Ethiopia*
[2]*Department of Metallurgical and Materials Engineering, College of Engineering, Defense University, Bishoftu 1041, Ethiopia*

Correspondence should be addressed to Mezigebu Belay; mezigebu848@gmail.com

Received 7 May 2023; Revised 19 June 2023; Accepted 13 July 2023; Published 25 July 2023

Academic Editor: Marta Fern ndez Garc a

Plastics are ubiquitous in our daily life. However, the use of petrochemical-based plastic as packaging materials causes the depletion of non-renewable resources, thereby leading to an increase in oil prices and economic crises. Moreover, these petrochemical plastics raise the issue of environmental pollution due to their non-biodegradability. Owing to this, there is a need to develop an alternative biodegradable and eco-friendly packing material. Agar, which is extracted from seaweeds, is one of the abundantly available polymers. However, moderate tensile strength and thermal stability restrict its application. As a step forward, agar/reduced graphene oxide (RGO) composites were prepared by *in situ* reduction of GO in the polymer matrix. The tensile strength of the composite was found to increase by 55% at 2% RGO loading. The electrical conductivity and thermal properties of the composite were also improved. The presence of conductivity suggested that apart from packaging, agar/RGO composites can also have potential applications as capacitor plates creating a supercapacitor and as electric field-induced wound healing material.

1. Introduction

The use of petro-chemical based plastics as packaging materials increases the issue of environmental pollution, global warming, and ecological problems owing to their non-biodegradability. This demands the need to develop biodegradable plastic materials. Bioplastics have been developed as alternatives to petrochemicals based plastics [1–5]. These materials have the advantage of biodegradability, ecological responsibility, and sustainability [5, 6]. However, many of the biodegradable plastics heavily depend on forest reserves and some even may affect food stock for their production. Agar is a natural and biodegradable polymer that neither causes deforestation nor effect the food supply [7]. It is a polysaccharide that is obtained from algae, which is found in seaweed [8]. Many researchers reported its potential application, such as packaging materials [7, 9–12]. Though agar is found abundantly in nature and does not cause deforestation and scarcity of food resources, its application is restricted by moderate mechanical strength and thermal stability. Different reinforcements have been attempted to improve the tensile strength of agar [7, 9–11]. Nevertheless, not much improvement in tensile strength was observed due to poor interfacial bonding between the agar and the filler. For this reason, graphene/agar composites were developed by *in situ* reduction of graphene oxide (GO) in the polymer matrix. A similar method was used in Refs. [13, 14].

Graphene, a two-dimensional planar sheet of sp^2 bonded single layer carbon atoms in honeycomb crystal lattice has remarkable properties, such as superior mechanical properties [15], high electron mobility [16–18], surface area [19], and thermal conductivity [20]. These properties make graphene an attractive filler for polymer composites. To harness the extraordinary properties of graphene in a composite, its layers must be fully exfoliated and homogeneously dispersed into the polymer matrix. In addition, good interfacial bonding between the graphene and polymer matrix is desired. However, the dispersion of pristine graphene in a polymer matrix is not individual and homogenous because of the high Van der Waals force among graphene sheets and with low compatibility of pristine graphene with most polymers. On the other hand, GO, unlike pristine graphene has highly

decorated oxygen-bearing functional groups [21–24], and hence can be dispersed and exfoliated in water [25], and proved good interfacial bonding with the matrix.

The preparation and characterization of reduced GO (RGO) by a separate reduction of GO and dispersing the RGO with chemicals has been reported in the previous work [26].

In this work, graphene–agar composites were developed simply by incorporating GO in the agar matrix with subsequent reduction of GO sheets in the polymer matrix. The role of graphene on tensile strength, thermal stability, and electrical conductivity was studied.

2. Materials and Methods

Graphite flake was purchased from Sigma–Aldrich (USA), whereas HNO_3, HCl, and H_2SO_4 were purchased from Avantor Performance Materials India Limited (Haryana, India). H_3PO_4 was purchased from LOBA Chemie, meanwhile, 30% H_2O_2 (w/v) was purchased from Fisher Scientific (India). Agar (gelling temperature 34°C–36°C, pH 6.0–7.0, dissolution in water at 85°C) was purchased from Hi Media, India, whereas $KMnO_4$ and Polyvinyl alcohol (PVA) (MW 85,000–124,000 g/mol, at 85% degree of hydrolysis) was obtained from S D FINE-CHEM LIMITED (India).

2.1. Preparation of GO. GO was prepared by the synthesis of GO [27]. Its preparation and characterization were reported in our previous paper publication [26]. The procedure, in brief, is given below.

2.2. Preparation of RGO/Agar Composites. One gram of agar was dissolved in the required amount of distilled water (DI) water at 90°C under constant stirring. 5% (w/w) of PVA concerning agar was added as a plasticizer and kept under stirring for half an hour. GO suspension was added as per the required percentage and ultrasonicated for 5 minutes. The solution was heated to 100°C. Then, hydrazine hydrate weighing 70% of the GO was added followed by the addition of liquor ammonia to increase the pH to 10 to increase the charge density [28]. Thermogravimetric analysis (TGA) was performed under nitrogen flow from 30°C to 600°C at a 10°C/minutes scanning rate using PerkinElmer STA 800. The reaction mixture was stirred at the same temperature for 5 hours. The solution was cooled to 60°C. The films were cast in a 140 mm Petri dish and dried at 40°C. 1%, 2%, 5%, and 10% RGO/agar (w/w) films were prepared by *in situ* reduction of GO.

2.3. Study for Degradation Behavior Test. Degradation in 5% formic acid was performed for 2% RGO and agar films at room temperature in polypropylene tubes for 20 hours. After 20 hours, the films were removed from formic acid and washed with DI water, dried in an oven at 60°C, and weighed. The amount of degradation (%D) was calculated by

$$\%D = \frac{W_o - W_f}{W_o} \times 100, \quad (1)$$

where W_o is the initial weight of the sample and W_f is the final weight of the sample.

The test was performed for three samples of each category.

2.4. Characterization. Fourier transform infrared (FTIR) spectra were performed within a frequency range of 400–4000 cm^{-1} using PerkinElmer Spectrum Version 10.03.06. Samples were prepared by grinding 20 mg of composite with 80 mg of KBr. X-ray diffraction (XRD) measurement was performed using a Bruker (D8 focus) X-ray diffractometer with Cu Kα radiation. The thickness of the samples was measured with digital micrometers, and tensile testing was performed with an Instron 3369-U2075 universal testing machine equipped with a load cell of 100 N following an ASTM method D 1708-59T, the test was done for a minimum of six samples for each composition. The swelling study was conducted by measuring the initial weight of the dried sample using a digital microbalance and immersing 20 mm × 20 mm pieces of films in DI water for 24 hours. The films were then removed and wiped with tissue paper, and the final weight of the film was measured. The water absorption or swelling ratio (SR) was determined by the following equation.

$$\mathrm{SR}(\%) = \frac{w_f - w_o}{w_o} \times 100, \quad (2)$$

where w_f and w_o represent the weight of the sample after and before immersion, respectively. TGA was performed under nitrogen flow at the temperature range of 30°C–600°C with a scanning rate of 10°C/minutes using PerkinElmer STA 800. The electrical conductivity was measured with the Keithley instrument using four probe techniques. The electrical resistance was obtained from the reciprocal of the slope of the I–V curve, and the conductivity of the sample was calculated using the equation

$$\sigma = \frac{1}{4.54RT}, \quad (3)$$

where R and T are the resistance and thickness of the samples.

3. Result and Discussion

3.1. Formation, Reduction, and Exfoliation of GO. The formation and exfoliation of GO were confirmed by X-ray diffraction (XRD) (Figure 1). The XRD peak from graphite appeared at $2\theta = 26.6°$, which corresponds to an interplanar spacing of 0.35 nm as shown in Figure 1. This peak shifted to a lower angle of $2\theta = 9.22°$, which leads to a larger interplanar spacing of 0.96 nm confirming an efficient oxidation. This large increase in the interplanar spacing was because of the good intercalation of oxygen between the layers, causing displacement of the planes. This peak disappeared in the composite, which confirmed the complete reduction and exfoliation of GO in the matrix [29]. In addition, the brown color of GO was turned into dark black after the addition of liquor ammonia, and hydrazine hydrate suggesting that deoxygenation of GO took place [30]. The formation

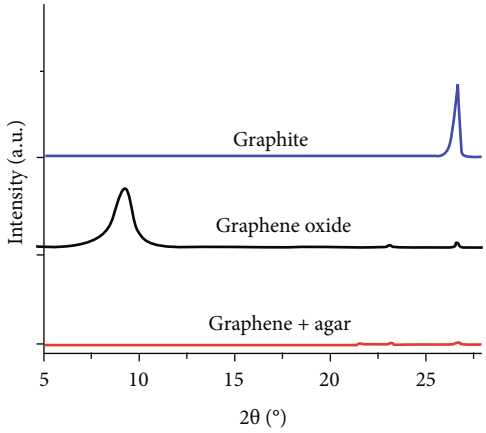

Figure 1: XRD of graphite, GO, and graphene/agar composite.

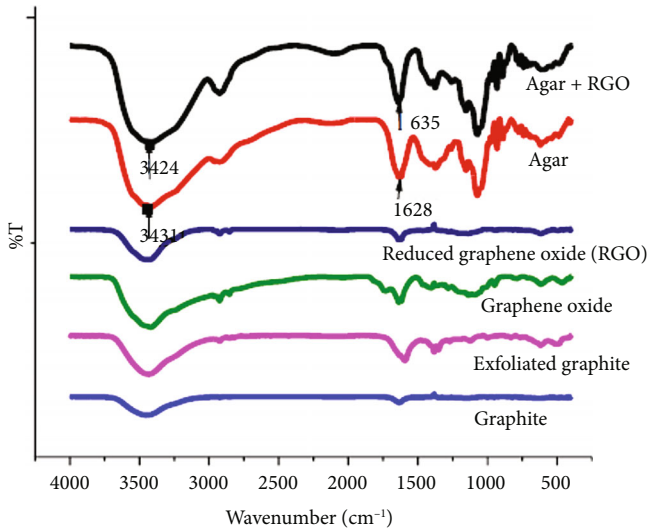

Figure 2: FTIR of graphite, exfoliated graphite, GO, graphene, agar, and grapheme/agar composite.

of GO, its exfoliation, and reduction were further characterized by FTIR, Raman spectroscopy, UV–Vis spectroscopy, TGA, Atomic Force Microscopy (AFM), and Transimision Electron Microcope (TEM), which was reported in our previous paper publication [26]. In addition, FTIR (Figure 2) was also used to confirm the interaction of the filler with the matrix. The –OH of agar at 3,431 cm^{-1} was shifted to a lower wave number 3,424 cm^{-1} in graphene/agar composites suggesting the existence of hydrogen bonding between the filler and the matrix [31].

3.2. Tensile Testing. The aim of incorporating RGO in a polymer matrix was to improve tensile strength and thermal stability. The addition of graphene in the polymer matrix has a significant effect on the tensile strength of polymers [30, 32, 33]. 1%, 2%, and 5% of RGO were used for tensile testing. However, 10% RGO/agar composites were not used for testing as the sample was brittle. The tensile strength of agar was 35.6 ± 4.7 MPa (Table 1) and (Figure 3). The incorporation of 2% by weight graphene increases the

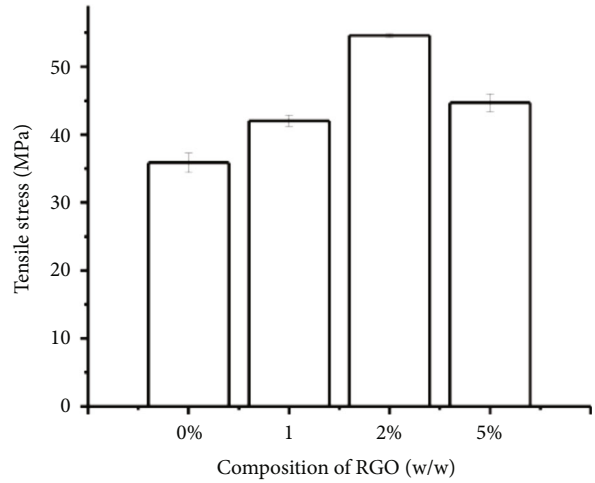

Figure 3: Effect of graphene content on tensile strength of agar.

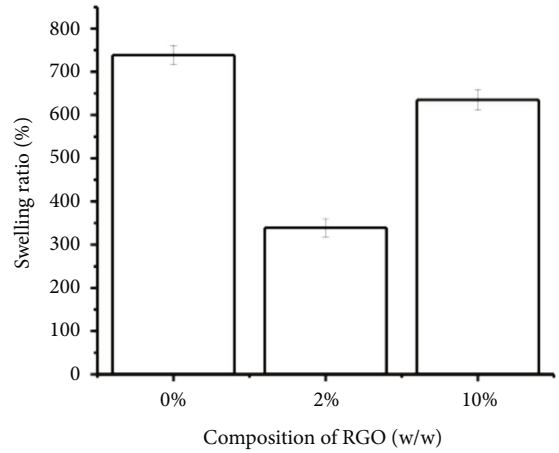

Figure 4: Effect of graphene content on SR of agar.

tensile strength of agar by 55%. This significant enhancement in tensile strength of the agar composite was due to the high aspect ratio [19], superior strength [15], homogeneous dispersion of graphene in the agar matrix [34], and strong interaction between the filler and the matrix. At a concentration higher than 2% the exfoliated graphene sheets could be well dispersed in the polymer matrix, leading to a significant enhancement in tensile strength. The decrease in tensile strength after 2% by weight RGO could be attributed to the decrease in the dispersion of the fillers at higher loading. When the critical concentration was reached and as the distance between the sheets became so small due to the strong Van der Waals force, the graphene sheets could be stacked together. Hence, at a concentration higher than 2% by weight, the nanosheets might stack together, decreasing the efficiency of the tensile strength improvement.

3.3. Water Absorption. Since 2% RGO and 10% RGO composites showed the highest and lowest strength. Swelling study was studied for 2% RGO and 10% RGO for comparison. The SR (Figure 4) showed that the incorporation of RGO reduces the

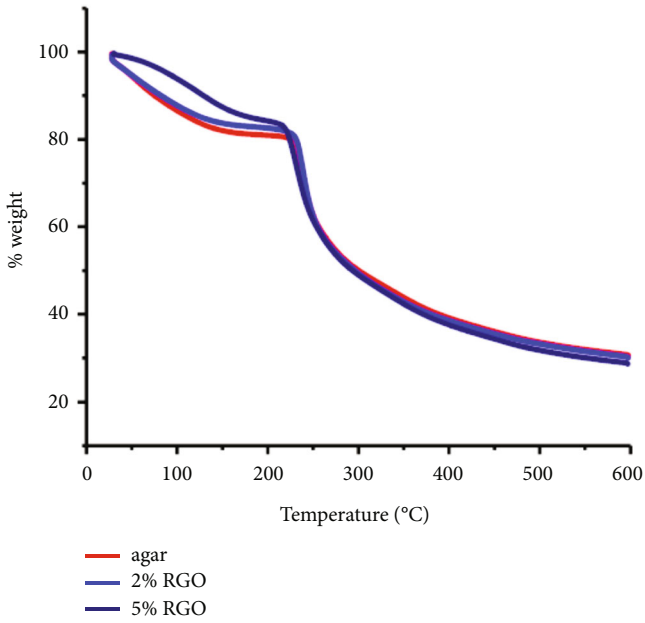

Figure 5: Effect of graphene content on thermal stability of agar.

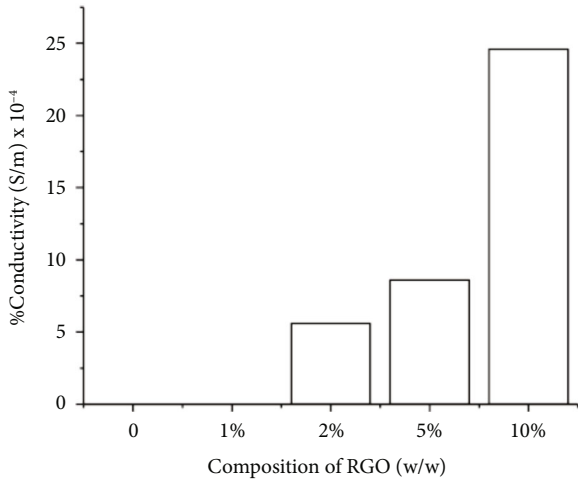

Figure 6: Effect of graphene content on electrical conductivity of agar.

water absorption of agar. Pure agar showed high SR (635%), whereas 2% RGO showed low water absorption (335%). The decrease in water absorption of agar by the incorporation of RGO could be due to the formation of hydrogen bonding by the residual hydroxyl group of the RGO and the hydroxyl group of the agar matrix thereby reducing the hydrophilicity of the polymer. Though the water absorption of agar was found to decrease at 2% RGO, it was found to increase at 10% RGO. The increase in water absorption at 10% RGO could be due to the agglomeration of RGO at higher loading creating poor interfacial bonding and void space, which could accommodate more water in it.

3.4. Thermal Stability. TGA was done for selectively for pure agar, 2% RGO and 5% RGO samples only. In the thermal

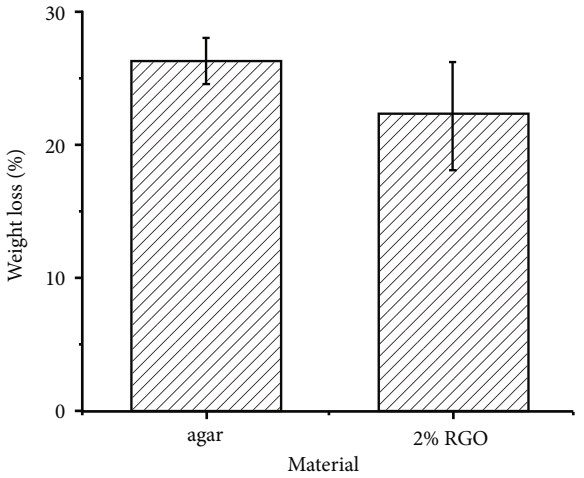

Figure 7: Effect of graphene on degradability of agar.

stability study, a sharp weight loss of 20% in agar and 15% in RGO/agar composites was observed in the service temperature ranging from 20°C to 200°C. This could be due to the liberation of unbound and bound water in the samples [35]. No weight loss was observed from 200°C to 230°C. Nevertheless, another sharp weight loss was observed from temperatures ranging from 230°C to 380°C. This could be due to the change in the physical and chemical properties of the materials [7].

The thermal stability (Figure 5) of RGO/agar composites had been improved to some extent with a service temperature ranging from 20°C to 200°C. This improvement might be ascribed to the stability of the hydrogen bond between the fillers and agar. However, not much change in the thermal stability of the composite was observed due to the absence of covalent bonding between RGO and agar. Moreover, since the concentration of graphene was low, it was not able to restrict the mobility of the polymer chain. Hence, no thermal stability was observed.

3.5. Electrical Conductivity. 0%, 1%, 2%, 5%, and 10% reduced oxide/agar films were used for electrical conductivity study. The electrical conductivity of agar and 1% RGO/agar (Figure 6) was below the detection limit of the instrument. Upon incorporation of graphene, the conductivity of the composite increased with the highest conductivity of 2.46×10^{-3} S/m at 10% by weight (mass fraction) graphene. Such improvement in electrical conductivity could be due to the large specific surface area and well dispersion of graphene in the matrix. The conductivity of the composite increased sharply at a concentration of 2% RGO due to the formation of a percolation threshold conductive network [36].

3.6. Observation of Degradation. The biodegradability of agar is available in the literature [7]. To study whether graphene affects the biodegradability of agar or not, a biodegradation behavior test was performed.

Since the tensile strength was maximum at 2% RGO. A degradation test was performed for 2% RGO and pure agar

Table 1: Summary of tensile strength and elongation at the break of graphene/agar.

Concentration of RGO (%)	Tensile strength (MPa)	Elongation at the break (%)
0	35 ± 4.7	12.3 ± 4.33
1	42 ± 4.2	7 ± 3.32
2	54.6 ± 2	13 ± 4.43
5	44.7 ± 2.9	5 ± 3.92

Note. The tensile strength values are means of tensile strength ± standard deviations (MPa) and the elongations (%).

to study the effect of graphene on the degradability of agar (Figure 7). It was observed that both agar and 2% reduced graphene composite were degradable, and the degradation behavior of agar was not affected much by the addition of graphene.

4. Conclusion

Graphene/agar composites were successfully synthesized by the incorporation of GO into agar matrix with subsequent reduction of GO to graphene sheets. The composite exhibited a significant improvement in tensile strength. The tensile strength of agar was improved by 55%, whereas its thermal stability also improved to some extent.

Data Availability

Data supporting this research article are available from the corresponding author or first author on reasonable request.

Conflicts of Interest

The author(s) declare(s) that they have no conflicts of interest.

Acknowledgments

The author would like to thank Dr. Vivek Verma and Dr. R. K. Nagarale for their valuable help.

References

[1] Y. Lu, L. Tighzert, F. Berzin, and S. Rondot, "Innovative plasticized starch films modified with waterborne polyurethane from renewable resources," *Carbohydrate Polymers*, vol. 61, no. 2, pp. 174–182, 2005.

[2] S. Z. Rogovina, "Biodegradable polymer composites based on synthetic and natural polymers of various classes," *Polymer Science, Series C*, vol. 58, no. 1, pp. 62–73, 2016.

[3] J. K. Pandey, A. P. Kumar, M. Misra, A. K. Mohanty, L. T. Drzal, and R. P. Singh, "Recent advances in biodegradable nanocomposites," *Journal of Nanoscience and Nanotechnology*, vol. 5, no. 4, pp. 497–526, 2005.

[4] J.-W. Rhim and P. K. W. Ng, "Natural biopolymer-based nanocomposite films for packaging applications," *Critical Reviews in Food Science and Nutrition*, vol. 47, no. 4, pp. 411–433, 2007.

[5] A. Sorrentino, G. Gorrasi, and V. Vittoria, "Potential perspectives of bio-nanocomposites for food packaging applications," *Trends in Food Science and Technology*, vol. 18, no. 2, pp. 84–95, 2007.

[6] X. Z. Tang, P. Kumar, S. Alavi, and K. P. Sandeep, "Recent advances in biopolymers and biopolymer-based nanocomposites for food packaging materials," *Critical Reviews in Food Science and Nutrition*, vol. 52, no. 5, pp. 426–442, 2012.

[7] A. Awadhiya, D. Kumar, and V. Verma, "Crosslinking of agarose bioplastic using citric acid," *Carbohydrate Polymers*, vol. 151, pp. 60–67, 2016.

[8] D. Phan The, F. Debeaufort, A. Voilley, and D. Luu, "Biopolymer interactions affect the functional properties of edible films based on agar, cassava starch and arabinoxylan blends," *Journal of Food Engineering*, vol. 90, no. 4, pp. 548–558, 2009.

[9] J.-W. Rhim, "Effect of clay contents on mechanical and water vapor barrier properties of agar-based nanocomposite films," *Carbohydrate Polymers*, vol. 86, no. 2, pp. 691–699, 2011.

[10] J.-W. Rhim, "Physical-mechanical properties of agar/κ-carrageenan blend film and derived clay nanocomposite film," *Journal of Food Science*, vol. 77, no. 12, pp. N66–N73, 2012.

[11] J. W. Rhim, L. F. Wang, and S. I. Hong, "Preparation and characterization of agar/silver nanoparticles composite films with antimicrobial activity," *Food Hydrocolloids*, vol. 33, no. 2, pp. 327–335, 2013.

[12] P. Kanmani and J.-W. Rhim, "Antimicrobial and physical-mechanical properties of agar-based films incorporated with grapefruit seed extract," *Carbohydrate Polymers*, vol. 102, pp. 708–716, 2014.

[13] Y. Chen, P. Pötschke, J. Pionteck, B. Voit, and H. Qi, "Smart cellulose/graphene composites fabricated by *in situ* chemical reduction of graphene oxide for multiple sensing applications," *Journal of Materials Chemistry A*, vol. 6, no. 17, pp. 7777–7785, 2018.

[14] W. Hu, S. Liu, Z. Wang, X. Feng, M. Gao, and F. Song, "*In situ* reduced graphene oxide and polyvinyl alcohol nanocomposites with enhanced multiple properties," *Frontiers in Chemistry*, vol. 10, article 856556, 2022.

[15] C. Lee, X. Wei, J. W. Kysar, and J. Hone, "Measurement of the elastic properties and intrinsic strength of monolayer graphene," *Science*, vol. 321, no. 5887, pp. 385–388, 2008.

[16] H. B. Heersche, P. Jarillo-Herrero, J. B. Oostinga, L. M. K. Vandersypen, and A. F. Morpurgo, "Bipolar supercurrent in graphene," *Nature*, vol. 446, no. 7131, pp. 56–59, 2007.

[17] S. V. Morozov, K. S. Novoselov, M. I. Katsnelson et al., "Giant intrinsic carrier mobilities in graphene and its bilayer," *Physical Review Letters*, vol. 100, no. 1, article 016602, 2008.

[18] K. S. Novoselov, A. K. Geim, S. V. Morozov et al., "Electric field effect in atomically thin carbon films," *Science*, vol. 306, no. 5696, pp. 666–669, 2004.

[19] M. D. Stoller, S. Park, Y. Zhu, J. An, and R. S. Ruoff, "Graphene-based ultracapacitors," *Nano Letters*, vol. 8, no. 10, pp. 3498–3502, 2008.

[20] A. A. Balandin, S. Ghosh, W. Bao et al., "Superior thermal conductivity of single-layer graphene," *Nano Letters*, vol. 8, no. 3, pp. 902–907, 2008.

[21] H. He, J. Klinowski, M. Forster, and A. Lerf, "A new structural model for graphite oxide," *Chemical Physics Letters*, vol. 287, no. 1-2, pp. 53–56, 1998.

[22] T. Nakajima, A. Mabuchi, and R. Hagiwara, "A new structure model of graphite oxide," *Carbon*, vol. 26, no. 3, pp. 357–361, 1988.

[23] A. Lerf, H. He, M. Forster, and J. Klinowski, "Structure of graphite oxide revisited," *The Journal of Physical Chemistry B*, vol. 102, no. 23, pp. 4477–4482, 1998.

[24] Y. Si and E. T. Samulski, "Synthesis of water soluble graphene," *Nano Letters*, vol. 8, no. 6, pp. 1679–1682, 2008.

[25] S. Park and R. S. Ruoff, "Chemical methods for the production of graphenes," *Nature Nanotechnology*, vol. 4, no. 4, pp. 217–224, 2009.

[26] M. Belay, R. K. Nagarale, and V. Verma, "Preparation and characterization of graphene-agar and graphene oxide-agar composites," *Journal of Applied Polymer Science*, vol. 134, no. 33, p. 45085, 2017.

[27] D. C. Marcano, D. V. Kosynkin, J. M. Berlin et al., "Improved synthesis of graphene oxide," *ACS Nano*, vol. 4, no. 8, pp. 4806–4814, 2010.

[28] D. Li, M. B. Muller, S. Gilje, R. B. Kaner, and G. G. Wallace, "Processable aqueous dispersions of graphene nanosheets," *Nature Nanotechnology*, vol. 3, no. 2, pp. 101–105, 2008.

[29] X. Yang, L. Li, S. Shang, and X.-m. Tao, "Synthesis and characterization of layer-aligned poly(vinyl alcohol)/graphene nanocomposites," *Polymer*, vol. 51, no. 15, pp. 3431–3435, 2010.

[30] X. Zhao, Q. Zhang, D. Chen, and P. Lu, "Enhanced mechanical properties of graphene-based poly(vinyl alcohol) composites," *Macromolecules*, vol. 43, no. 5, pp. 2357–2363, 2010.

[31] L. Lu, H. Sun, F. Peng, and Z. Jiang, "Novel graphite-filled PVA/CS hybrid membrane for pervaporation of benzene/cyclohexane mixtures," *Journal of Membrane Science*, vol. 281, no. 1–2, pp. 245–252, 2006.

[32] J. Liang, Y. Huang, L. Zhang et al., "Molecular-level dispersion of graphene into poly(vinyl alcohol) and effective reinforcement of their nanocomposites," *Advanced Functional Materials*, vol. 19, no. 14, pp. 2297–2302, 2009.

[33] X. Wang, H. Bai, Z. Yao, A. Liu, and G. Shi, "Electrically conductive and mechanically strong biomimetic chitosan/reduced graphene oxide composite films," *Journal of Materials Chemistry*, vol. 20, no. 41, pp. 9032–9036, 2010.

[34] X. S. Du, M. Xiao, Y. Z. Meng, and A. S. Hay, "Direct synthesis of poly(arylenedisulfide)/carbon nanosheet composites via the oxidation with graphite oxide," *Carbon*, vol. 43, no. 1, pp. 195–197, 2005.

[35] A. A. Apostolov, S. Fakirov, E. Vassileva, R. D. Patil, and J. E. Mark, "DSC and TGA studies of the behavior of water in native and crosslinked gelatin," *Journal of Applied Polymer Science*, vol. 71, no. 3, pp. 465–470, 1999.

[36] V. H. Pham, T. T. Dang, S. H. Hur, E. J. Kim, and J. S. Chung, "Highly conductive poly(methyl methacrylate) (PMMA)-reduced graphene oxide composite prepared by self-assembly of PMMA latex and graphene oxide through electrostatic interaction," *ACS Applied Materials and Interfaces*, vol. 4, no. 5, pp. 2630–2636, 2012.